Correction of ADCP Compass Errors Resulting from Iron in the Instrument's Vicinity*

Wilken-Jon von Appen

Helmholtz Centre for Polar and Marine Research, Alfred Wegener Institute, Bremerhaven, Germany

ABSTRACT

Iron in the vicinity of compasses results in compass deviations. ADCPs mounted on steel buoyancy devices and deployed on seven moorings on the East Greenland outer shelf and upper slope from 2007 to 2008 suffered from severe compass deviations as large as 90°, rendering the ADCP data useless without a compass correction. The effects on the measured velocities, which may also be present in other oceanic velocity measurements, are explained. On each of the moorings, velocity measurements from a different instrument are overlapping in space and time with the compromised measurements. The iron was not in the vicinity of this second instrument, and the instrument is therefore assumed not to be affected by compass deviations. A method is described to determine the compass deviation from the compromised and uncompromised velocity measurements, and the compromised compass headings. The method depends on the assumptions that at least one instrument per mooring is not compromised and that the change in flow direction over the vertical distance from the compromised to the uncompromised velocity measurement is zero on average. With this method, the compromised headings and the compromised velocity records can be corrected. The method is described in detail and a MATLAB function implementing the method is supplied. The success of the method is demonstrated for a mooring with a minor compass deviation and for one with a large amplitude deviation.

1. Introduction

Steel can exhibit two different magnetic behaviors related to the iron it contains: Magnetically hard iron keeps the magnetic field that had been imparted on it during its formation (e.g., when it cooled from the liquid phase). Soft iron, on the other hand, allows its magnetic dipoles to align with the ambient magnetic field (e.g., the earth's magnetic field). Compasses point in the direction of the ambient magnetic field, which is the sum of the earth's magnetic field and the magnetic field of any iron (both hard and soft) in addition to other magnetic materials and electromagnets present. If a significant amount of iron is in the vicinity of a compass, the direction in which the compass will point may be substantially different from magnetic north (as indicated by the field lines of the earth's magnetic field). The error due to this effect can be as large as the full range of achieved instrument headings.

A common setup in oceanographic moorings is to have an ADCP mounted on a buoyancy device. The ADCP may be looking up or down from its location in the mooring. Syntactic foam spheres contain a small amount of steel (and hence iron) and are comparably expensive. Steel spheres, on the other hand, are more economical (approximately half the price of syntactic foam spheres) but, by design, they contain large amounts of iron. The setup as shown in Fig. 1, where the ADCP is attached to the sphere and is hence separated by less than 0.5 m, was employed in a mooring deployment in 2007. Since an integral component of any velocity measurement is the determination of the instrument orientation using its compass, the compass deviation due to the iron in the vicinity has a direct effect on the velocity measurements. There are likely many mooring setups in which this introduces small errors in the velocity measurements, but there are also several mooring setups where the resulting errors are large.
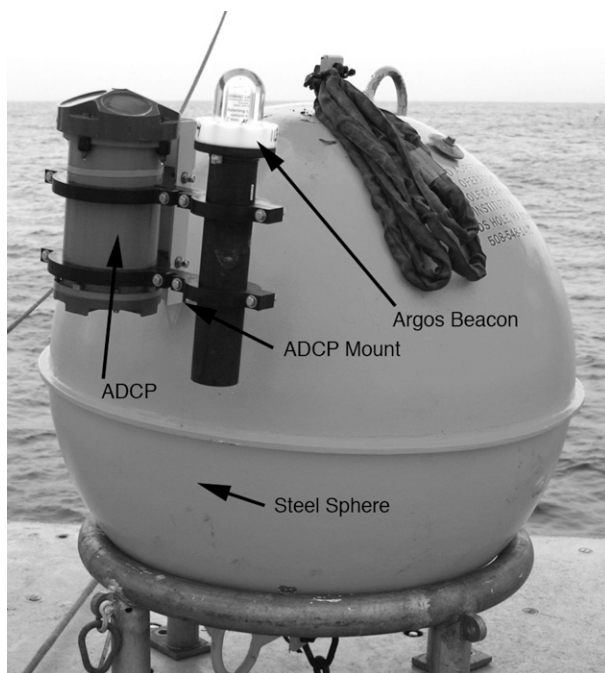
FIG. 1. The mooring setup discussed in this paper prior to deployment at sea. The upward-facing ADCP and the Argos beacon are attached to the steel sphere using a mount. (Photo by Daniel Torres, Woods Hole Oceanographic Institution.)

Precruise and/or postcruise calibration on land of the ADCP compass is advisable, but it may not be sufficient to deal with this problem. The effects of hard steel can be dealt with using such a calibration, but the behavior of the soft steel may be significantly different if the absolute magnitude of the earth's magnetic field and/or the ratio of its horizontal to its vertical component is significantly different between the deployment location and the calibration location on land. This would be specifically applicable for deployments at high latitude (in the Arctic or Antarctic) and calibration at lower latitudes.

In the deployment of an array of seven moorings across the East Greenland outer shelf and upper continental slope, a particularly bad case of this compass deviation was encountered. The order of magnitude of this effect was that for the full 360° that each of the compasses on the moorings should have recorded for at least a very short time during the deployment year, some ADCP compasses only ever measured directions within a 100° range. This means that the other 260° of possible directions received zero counts.[1] However, the moorings also contained

a second instrument [an ADCP on some of the moorings and an acoustic current meter (ACM) on the other moorings] measuring velocities from an instrument location that was at least several meters removed from the steel spheres. Some of the velocity measurements from the two instruments were spatially and temporally in close proximity. In the following, we assume that the compass of the lower instrument was not affected by the steel sphere. This assumption cannot be explicitly verified. However, there are no indications in the records to suggest that they were affected (the full 360° of compass headings were recorded). Furthermore, the resulting scientific results (e.g., Harden et al. 2014; von Appen et al. 2014a,b) are self-consistent and consistent with previous studies of the dynamics in the region based on shipboard surveys, sea surface temperature observations, numerical models, and theory. This provides confidence that the assumption that the lower instruments are not affected is correct.

This paper documents a method that uses theory about compass deviations together with the overlapping velocity measurements to correct the ADCP velocities. While it is not clear how often this specific setup has occurred elsewhere, we believe that the current approach may be helpful to improve the data quality of other ADCP records compromised in a similar manner as long as some independent information about the flow field measured by the compromised instrument exists. One such setup might be a lowered ADCP mounted on a CTD rosette under the influence of the steel in the rosette frame and the attached weights. In this case, measurements from a vessel-mounted ADCP may be used as an independent uncompromised record of the overlapping ocean current velocities to correct the compass deviation of the lowered ADCP's compass. This correction would precede the conventional processing step of applying vessel-mounted ADCP measurements as a constraint to the inversion of lowered ADCP data.

2. Description of the mooring setup

From 4 September 2007 to 4 October 2008, seven moorings were deployed across the outer shelf and upper continental slope of East Greenland between 65°30.0′N, 33°8.8′W and 65°7.3′N, 32°41.1′W. The exact mooring positions and instrument configurations are provided in Table 1 and a cross-sectional view of the mooring array is shown in Fig. 2. EG4 (the fourth mooring) contained the largest number of individual instruments and its design is shown in Fig. 3. The other moorings were identical, except that they were missing some of the instruments as detailed in Table 1 and that

---

[1] We note that similar effects (compass ranges of only ≈100°) can also result from incorrect lookup tables in the instruments' firmware. If the resulting biases are only heading dependent, then the methods described in this paper could also be applied in those situations.

TABLE 1. The following mooring details are given: name of mooring, latitude, longitude, and water depth of the moorings; and the type, the approximate instrument depth, and the approximate measuring range of the upper ADCPs and the lower current meters.

			Upper ADCP			Lower current meter		
Name	Latitude/ Longitude	Water depth (m)	Type	Instrument depth (m)	Measuring range (m)	Type	Instrument depth (m)	Measuring range (m)
EG1	65°30.0′N 33°8.8′W	248	Upward-facing 300-kHz ADCP	100	20–92	Upward-facing 300-kHz ADCP	248	100–240
EG2	65°26.6′N 33°4.5′W	268	Upward-facing 300-kHz ADCP	100	20–92	Upward-facing 300-kHz ADCP	268	100–260
EG3	65°23.2′N 33°1.0′W	524	Upward-facing 300-kHz ADCP	100	20–92	Upward-facing 75-kHz ADCP	524	100–514
EG4	65°20.0′N 32°57.3′W	894	Upward-facing 300-kHz ADCP	100	20–92	Downward-facing 75-kHz ADCP	104	114–450
EG5	65°16.2′N 32°52.7′W	1163	Upward-facing 300-kHz ADCP	100	20–92	ACM/MMP	—	102–1158
EG6	65°12.3′N 32°47.0′W	1378	Upward-facing 300-kHz ADCP	100	20–92	ACM/MMP	—	102–1373
EG7	65°7.3′N 32°41.1′W	1585	Upward-facing 300-kHz ADCP	100	20–92	ACM/MMP	—	102–1580

the 5/16-in. Jac Nil Wirerope was a different length to achieve the position of the steel sphere at ≈100-m depth. All of the moorings were designed to measure velocity between the bottom and the surface. At each of the moorings, a top buoyancy sphere made of steel was moored in ≈100-m depth and an upward-looking 300-kHz Teledyne RD Instruments (RDI) Workhorse ADCP was attached to the sphere. Figure 1 shows a photo of how the ADCP was attached to the sphere. Upward-looking 300-kHz RDI Workhorse ADCPs were moored on the bottom of EG1 and EG2. EG3 and EG4 had upward-looking 75-kHz RDI Long Ranger ADCPs on the bottom, and EG4 also had a downward-looking 75-kHz RDI Long Ranger ADCP attached to the mooring cable >1 m below the steel sphere. McLane Moored Profilers (MMPs) containing a Falmouth Scientific Inc. (FSI) ACM each operated between the bottom and the steel sphere on EG5–EG7. The profilers on EG5–EG7 therefore measured velocity as well as conductivity/temperature/pressure. Instead of the MMPs, EG1–EG4 had coastal moored profilers (CMP; a Woods Hole Oceanographic Institution in-house development) that only measured conductivity/temperature/pressure.

This means that at all moorings, velocity was measured closely above the steel spheres by the first bin of the attached upward-looking ADCPs and closely below. On EG1–EG3, the measurement below was achieved by the distant bins of the upward-looking ADCPs and on EG4 by the first bin of the downward-looking ADCP. On EG5–EG7, the measurement below was achieved by the MMPs when they were near their top bumper stop. While we realize that there is shear and short-term

temporal variability, we considered measurements above and below the sphere separated by less than 20 min in time and 20 m in the vertical to be overlapping. These overlapping velocity measurements should, on average, measure the same flow speed and direction. This is one assumption used in this paper, and the second assumption is that the lower instruments were not affected by compass deviations.

The currents on the upper continental slope turned out to be stronger than anticipated during the design of
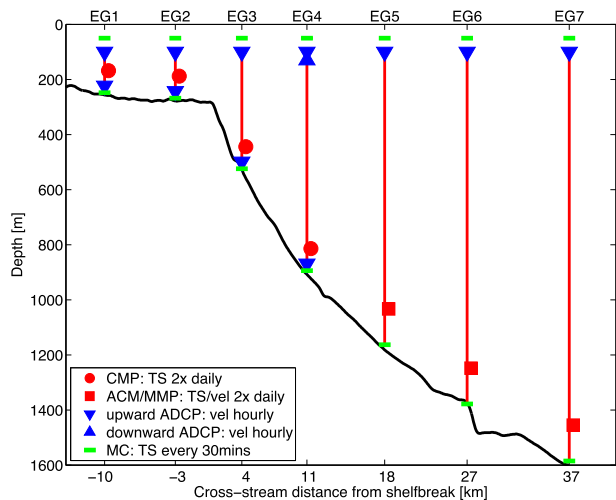

FIG. 2. Cross-sectional view of the East Greenland mooring array. The different instruments and their sampling schedules are explained in the legend. The nominal depth range sampled by the CMPs and MMPs is shown in red. The bottom depth along the mooring line, measured by the ship's echo sounder, is shown in black. MC: Microcat. (Figure from von Appen et al. 2014b.)
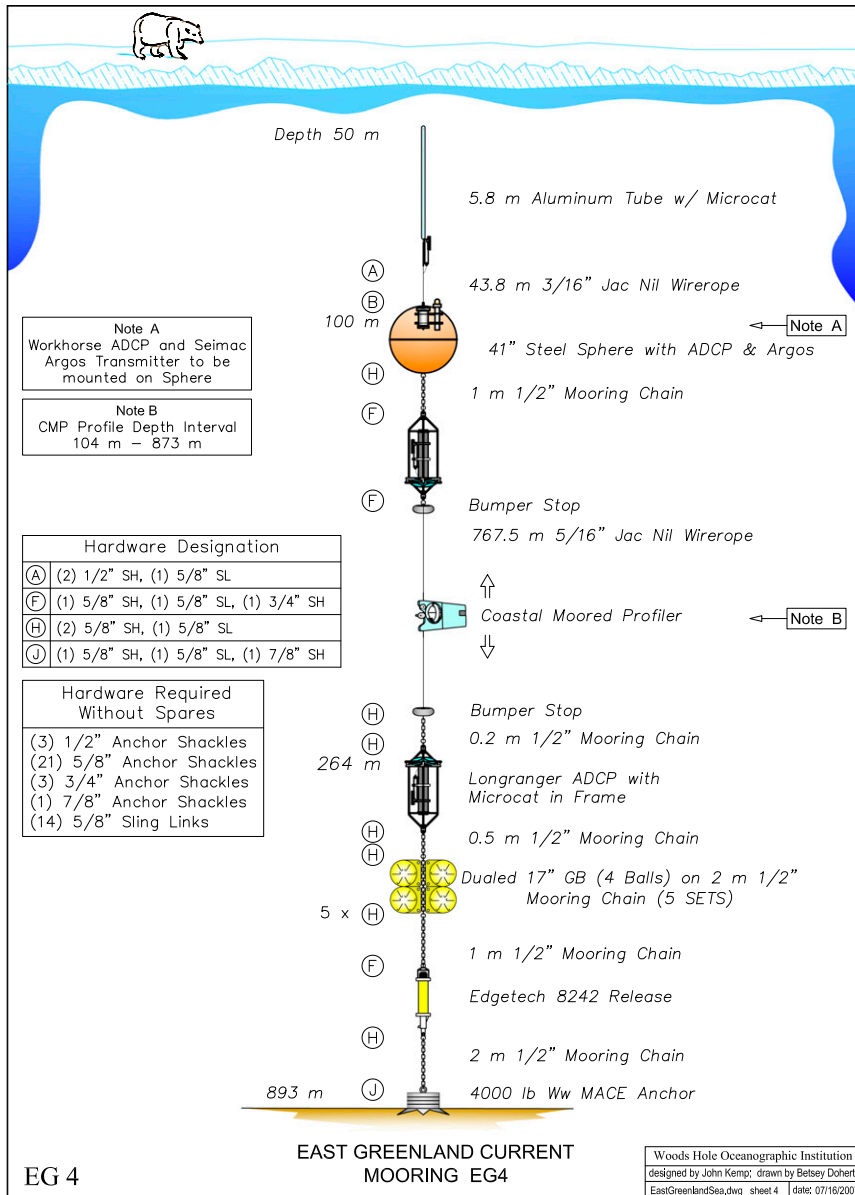
FIG. 3. Diagram of mooring EG4. The distances in the vertical are not to scale, but the wire lengths are indicated instead. The other moorings were similarly designed, but, as detailed in the text, they were missing some instruments compared to EG4. No swivels were used in the moorings. (Figure designed by John Kemp and drawn by Betsey Doherty, Woods Hole Oceanographic Institution.)

the moorings. This resulted in frequent large amplitude mooring motion. Some of the top buoyancy spheres were blown down from their target water depth of 100 m to more than 400-m depth. This complicated the interpretation of the data and also caused the moored profilers to miss profiles, as they were stuck during strong blowdown events, but it also allowed for the identification of large velocity events associated with the passage of Denmark Strait Overflow Water cyclones

(von Appen et al. 2014b). However, because the steel sphere is at the top of the mooring, the tilt (combined roll and pitch) of the upward-looking top ADCPs never exceeded 10° and was typically around 5°. Since these tilt values are not atypically large and because the compass deviation also occurred on the shallowest mooring EG1, which—being on the shelf—was not subject to significant blowdowns, we conclude that the compass deviation is not related to the blowdowns.
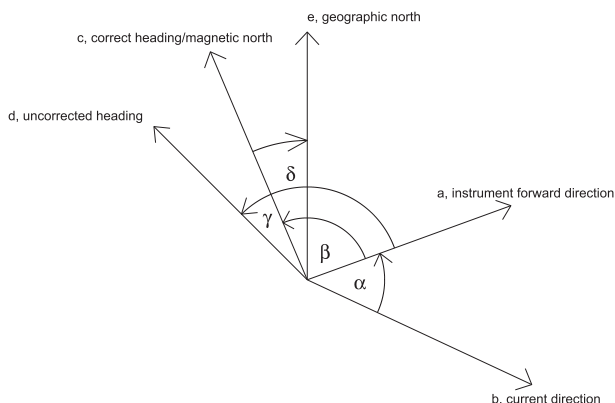
FIG. 4. Definition sketch of the directions and angles mentioned in the text.

3. Theory of magnetic compass deviation

The combined effects of different configurations of iron in the vicinity of a compass lead to a compass deviation. A compass deviation is the difference between the correct heading to magnetic north and the uncorrected heading recorded by the compass. This compass deviation is a function of the direction with respect to magnetic north. The geometry of the iron in the vicinity of the compass can be decomposed into a symmetric and an asymmetric part (National Geospatial-Intelligence Agency 2004).[2] Geometrical considerations show that any geometry can, in general, be described as the sum of these two parts. The two parts have different influences on the compass, but their sum has a special functional form with only five independent parameters:

$$\beta - \gamma(\beta) = A + B\sin(\beta) + C\cos(\beta) + D\sin(2\beta) + E\cos(2\beta). \qquad (1)$$

Here β is the correct heading to magnetic north and γ is the uncorrected heading of the compass needle as defined in Fig. 4. Following National Geospatial-Intelligence Agency (2004), the constant A is a bias resulting from physical misalignments of the compass. The coefficients B and C associated with the semicircular sin (β) and $\cos(\beta)$, respectively, describe the effects of the permanent magnetic field of hard iron. Finally, induced magnetism from soft iron contributes to all five coefficients, A, B, C, D, and E. As such it is not possible to conclude from a particular compass deviation curve whether hard or soft iron effects dominate. The

remainder of this paper derives a method to determine these five constants and to then use them to correct the compass headings.

Mechanisms developed to correct the compass deviation due to such steel geometries are typically applied to ships' compasses (e.g., National Geospatial-Intelligence Agency 2004), as they treat ships as sums of symmetric and asymmetric arrangements of hard and soft steel in the vicinity of the compasses. A steel sphere in the vicinity of an ADCP is nothing else. Therefore, we consider the theory developed for ships to be also applicable for ADCPs in the vicinity of steel spheres. Note that this assumes that the ship or steel sphere does not roll or pitch. Roll and pitch lead to a tilting of the steel arrangement relative to the earth's magnetic field. The coefficients A–E do not account for the effect of tilt. We justify this omission by the fact that, since the ADCP was at the top of the moorings, the instrument tilt was recorded to be small (between 3° and 10°). The compass heading error due to these values of the tilt is an order of magnitude smaller than the effects of the iron.

Just as in a ship, there is a forward direction to an ADCP. The ADCP measures currents in the instrument's reference frame (instrument coordinates) for which, by convention, beam 3 is forward. Using beam 3 as the instrument forward direction, β (beta) is the ADCP's corrected heading (Fig. 4) and γ (gamma) is the uncorrected heading (relative to magnetic north). Any differences between β and γ are due to compass errors. Figures 5a, 6a, and 7a show this pointing error (compass deviation) as a function of the beam 3 direction. Figure 5 shows a range of synthetically constructed compass deviations with differing amplitudes. Figure 6 shows real data from mooring EG2 for a case with a small compass deviation and Fig. 7 shows data from EG4 with a large amplitude compass deviation case.

For the following discussion, we introduce a few directions and angles, all of which are defined with respect to the ADCP's forward direction and sketched in Fig. 4:

- a: Forward direction of ADCP, beam 3 pointing direction.
- b: Current direction, direction in which the water is moving.
- c: Magnetic north, the heading of a correctly compensated compass.
- d: Direction in which an uncorrected compass points.
- e: Geographic north, lines of constant longitude.[3]

---

[2] This handbook (National Geospatial-Intelligence Agency 2004) provides useful background and details about compass corrections, as they are standard on ships.

[3] The equivalent terms used in the handbook of the National Geospatial-Intelligence Agency (2004) are "ship's heading" for a, "magnetic meridian" for c, and "true meridian" for e.

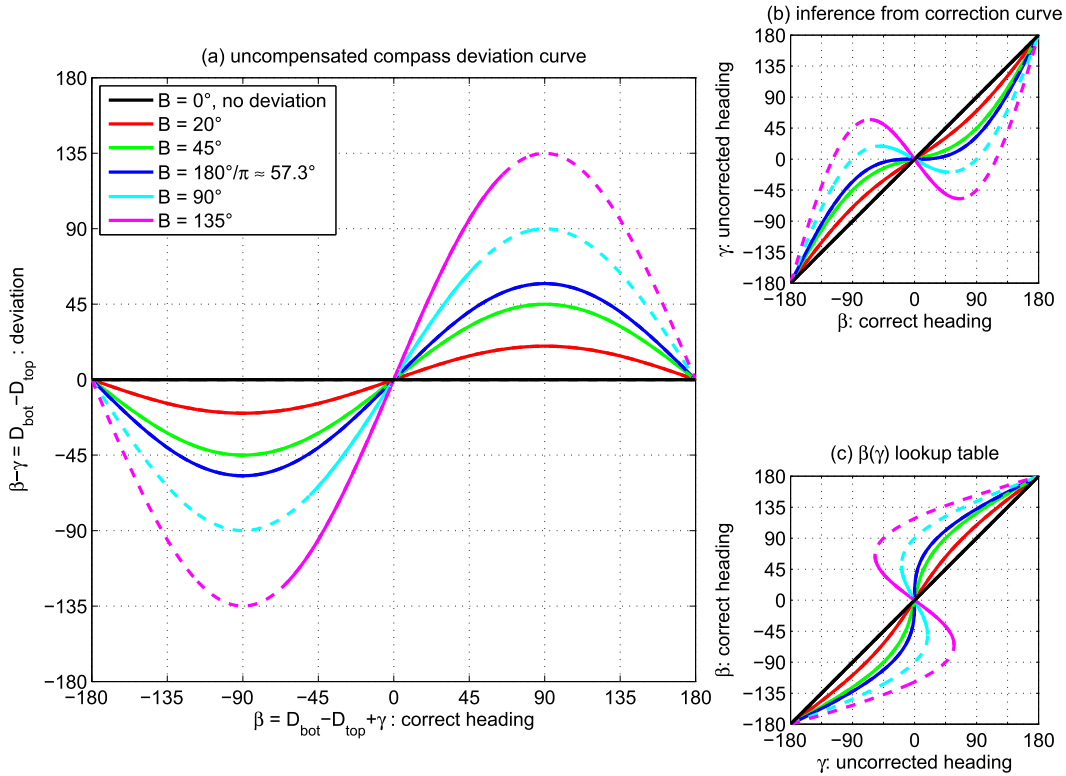FIG. 5. Synthetic compass deviation curves. A, C, D, and E of Eq. (1) are set to zero and B varies, as shown in the legend of (a). (a) The uncompensated compass deviation curve, (b) the inference from the fitted correction curve, and (c) the lookup table for $\beta(\gamma)$. The curves are solid where they can be inverted and dashed elsewhere.

- α: Angle between b and a, current direction in instrument coordinates.
- β: Angle between a and c, correct heading to magnetic north in instrument coordinates.
- γ: Angle between a and d, uncorrected ADCP compass heading. This is what the ADCP incorrectly records as its magnetic heading. Note that this does not yet account for the declination δ, which is only applied during processing on shore after the recovery.
- δ: Angle between c and e, declination, also known as variation. This is the difference between the directions to magnetic north and geographic north. For oceanographic purposes, it is a known geophysical external parameter that for any location and time on Earth can be retrieved from a numerical model (such as http:// ngdc.noaa.gov/geomag/magfield.shtml).

The quantities measured during the deployment with two overlapping instruments as described in the previous section can be expressed in terms of the above-defined directions and angles:

- γ: Uncorrected heading of upper ADCP.

- D_{bot}: Current direction of lower ADCP/ACM after onshore processing, including correction for magnetic declination δ. This current direction measurement is assumed not to be affected by a compass deviation.
- $D_{top} = \alpha + \gamma + \delta$: Current direction of upper ADCP after onshore processing that was affected by a compass deviation.

The correct current direction of the upper ADCP would be $D_{top}^{corr} = \alpha + \beta + \delta$. But if, as assumed, the records from the two instruments are overlapping, then the correct current directions from the two instruments should be identical, that is, $D_{top}^{corr} = D_{bot}$.

The following quantities are needed to construct the compass deviation curve as defined in Eq. (1):

- *Forward direction of upper ADCP* in correct magnetic Earth coordinates:

$$\beta = (\alpha + \beta + \delta) - (\alpha + \gamma + \delta) + \gamma$$
$$= D_{top}^{corr} - D_{top} + \gamma = D_{bot} - D_{top} + \gamma. \quad (2)$$

- *Compass deviation* (magnetic deviation of compass due to the presence of iron in its vicinity):
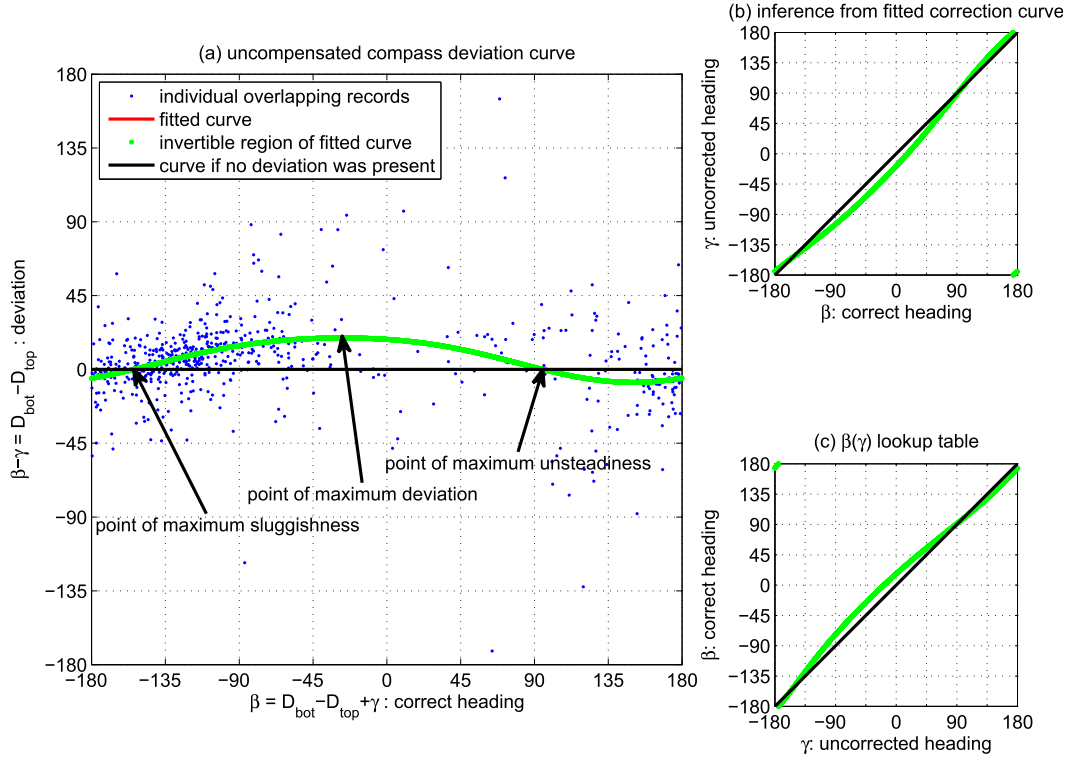
FIG. 6. Analysis plots for the compass correction of the ADCP on EG2, which exhibited only a minor compass deviation. (a) The uncompensated compass deviation curve, (b) the inference from the fitted correction curve, and (c) the lookup table for $\beta(\gamma)$. The black line would apply if there were no compass deviation. Note that since the deviation is minor, the fitted curve can be inverted over the full range of uncorrected headings, which is why the red curve is identical to—and covered by—the green curve. Note that the plotting limits of the periodic x axis are chosen to best fit the data scatter into the interior of the figure.

$$\beta - \gamma = (\alpha + \beta + \delta) - (\alpha + \gamma + \delta)$$
$$= D_{\mathrm{top}}^{\mathrm{corr}} - D_{\mathrm{top}} = D_{\mathrm{bot}} - D_{\mathrm{top}}. \qquad (3)$$

To illustrate the results of compass deviations, Fig. 5 shows synthetic compass deviation curves. To keep the discussion simple, we considered only a simplified version of Eq. (1), where A, C, D, and E are set to zero and B varies over a range of typical values.

The mapping from the correct magnetic compass direction to the compass deviation is called the uncompensated compass deviation curve $\beta \to \beta - \gamma$ and is shown in Fig. 5a for the synthetic cases. There are two special regions on the compass deviation curve. The compass behavior is "sluggish," where for a given change in correct instrument heading β, the uncorrected heading γ changes by a smaller amount, that is, $(\partial\gamma/\partial\beta) < 1$ (National Geospatial-Intelligence Agency 2004). Conversely, the behavior is "unsteady" in the region where γ changes by a larger amount than β: $(\partial\gamma/\partial\beta) > 1$. In the example, the sluggish region is in the vicinity of $\beta = 0°$ (Fig. 5b), while the unsteady region is near $\beta = \pm 180°$.

When the uncompensated compass deviation curve $\beta \to \beta - \gamma$ has been constructed, the relationship between correct and uncorrected heading can be plotted as $\beta \to \gamma$ and then inverted as $\gamma \to \beta$. If the compass deviations are of large amplitude, the response of the compass changes sign; that is, for an increase in the uncorrected heading, the correct heading actually decreases: $(\partial\gamma/\partial\beta) < 0$. In the synthetic case, this happens for values of B larger than $180°/\pi \approx 57.3°$. In those cases, the inversion is no longer unique and $\beta(\gamma)$ becomes multivalued. In this case, the inversion can only be carried out in the region of maximum sluggishness and the lookup table $\beta(\gamma)$ will not be defined for all uncorrected headings γ.

To see the effect of the compass deviations shown in Fig. 5 on the measured velocities, consider the velocity that is recorded by the instrument for an ocean velocity that is aligned with the forward direction of the instrument, that is, $\alpha = 0$. For simplicity, we also assume $\delta = 0$ here. For a correct heading of $0°$, all of the synthetic compass deviations would not affect the recorded ocean current directions and they would always correctly be
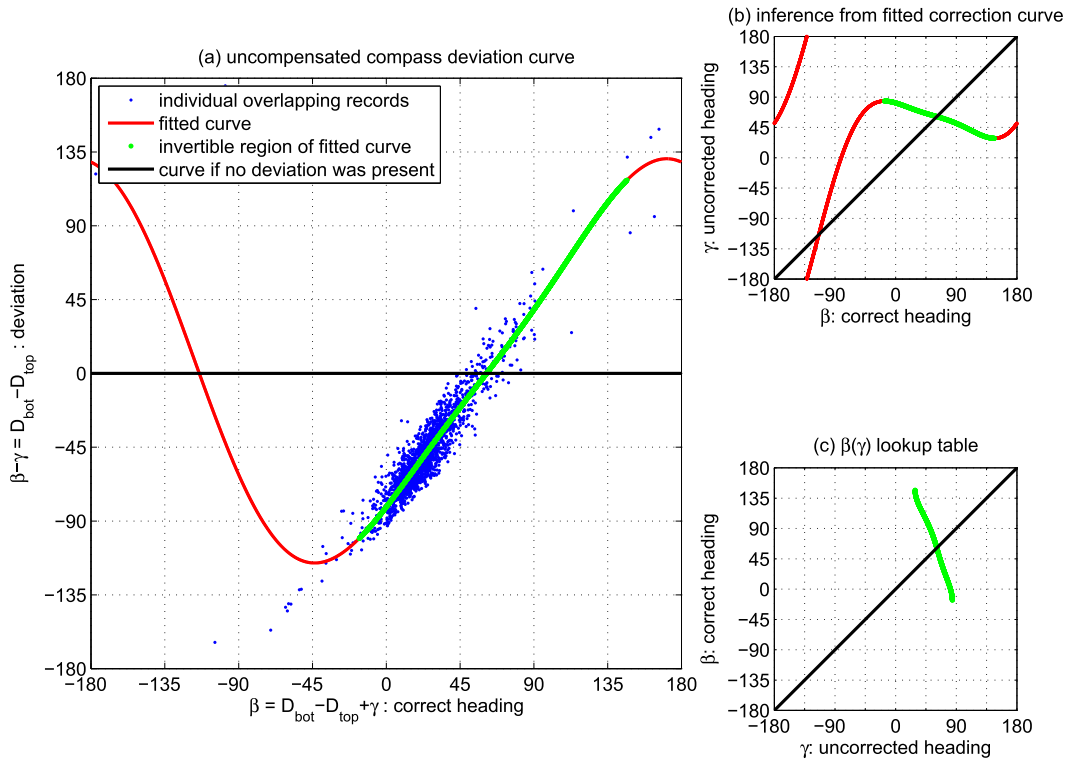
FIG. 7. As in Fig. 6, but for EG4, which exhibited a large amplitude compass deviation. Note that the fitted curve can be inverted only in a small range (29°–84°) of uncorrected headings.

recorded as 0°. However, for the same $\alpha = 0$ and a correct heading of $\beta = 90°$, the recorded velocities would be $\alpha + \gamma + \delta = \alpha + \beta - (\beta - \gamma) + \delta = 90° - B$. The synthetic compass deviations with amplitudes of $B = 0°$, 20°, 45°, 57.3°, 90°, and 135° would result in recorded current directions of 90°, 70°, 45°, 33.7°, 0°, and −45°, respectively, which clearly would be disastrously different from the correct current direction of 90° for any compass deviation much bigger than 20° in amplitude.

However, if $\beta(\gamma)$ (the correct heading β corresponding to the uncorrected heading γ) can be determined, then the ADCP compass can be corrected in order to obtain the *corrected upper current direction:*

$$D_{\text{top}}^{\text{corr}} = \alpha + \beta(\gamma) + \delta = (\alpha + \gamma + \delta) + \beta(\gamma) - \gamma$$
$$= D_{\text{top}} + \beta(\gamma) - \gamma. \qquad (4)$$

A lookup table for $\beta(\gamma)$ must be constructed. For the γ for which $\beta(\gamma)$ is defined, the upper current direction can be corrected, while it is not possible for the γ for which $\beta(\gamma)$ is not defined and those current directions must be marked as not a number (NaNs). The correction according to Eq. (4) can be applied to any extended dataset from the upper ADCP and is not limited to the overlapping times and depths.

4. Application of method to mooring data

The correction method involves the following steps, which have been implemented in a MATLAB function that is supplied in the supplemental online material (http://dx.doi.org/10.1175/JTECH-D-14-00043.s1) and described in the appendix.

- Construct a scatterplot based on the overlapping measurements of $\beta \rightarrow \beta - \gamma$.
- Use the MATLAB curve fitting toolbox to fit a smooth line obeying Eq. (1) to the scatter. This might, for example, also be done with Python's scipy.optimize. curve_fit package.
- Use the fitted curve of $\beta \rightarrow \beta - \gamma$ to plot $\beta \rightarrow \gamma$.
- If the compass deviation is of small amplitude such that $\gamma \rightarrow \beta$ is not multivalued, invert the curve and plot it.
- If the compass behaves very sluggish (only a smaller range of headings than the expected range was recorded), then the same compass deviation γ can refer to different correct headings β and $\beta \rightarrow \gamma$ becomes multivalued. The greatest information is then contained in the region of maximum sluggishness. This region has to be selected for the inversion.
- Invert the curve in the sluggish region (around the minimum of $\partial\gamma/\partial\beta$).

- The lookup table of $\beta(\gamma)$ has been achieved and can be used to correct the upper current direction: $D_{top}^{corr} = D_{top} + \beta(\gamma) - \gamma$.
- To assess the success of the compass correction, plot histograms of the upper uncorrected and the upper corrected headings along with histograms of the upper uncorrected, the upper corrected, and the lower current directions. A scatter of the upper uncorrected and corrected directions versus the lower current direction allows for an assessment of how much the correlation has improved.

The method has been applied successfully to all seven moorings on the East Greenland shelf and slope. For illustrative purposes, we present a case with only a minor compass deviation (mooring EG2) and a case with a large amplitude compass deviation (mooring EG4). The uncompensated compass deviation curve $\beta \rightarrow \beta - \gamma$ for EG2 (Fig. 6a) is constructed as a scatterplot of all the overlapping data points. These are defined as the measurements from the upper and lower instrument that were separated by less than 20 min in time and less than 20 m in the vertical. In the case of EG2, the compass deviation is small and therefore most of the data points are within 45° of 0°. The scatter is due to the slight offset in measurement time and location, noise, and other nonsystematic measurement errors. For mooring EG4, the compass deviation is large and the data scatter (Fig. 7a) therefore does not cluster around 0°. A nonlinear least squares fit to Eq. (1) is applied to the data scatter, resulting in the red curve. As the curve is invertible for all correct headings β, in the small compass deviation case (Fig. 6a), the red curve is overlaid by the green curve, indicating the invertible region. To find the region where the fitted compass deviation curve can be inverted, the correct heading β is subtracted from the fit and plotted versus the correct heading β (Figs. 6b and 7b). The inversion from $\beta \rightarrow \gamma$ to $\gamma \rightarrow \beta$ in the small amplitude case is straightforward as it is everywhere defined (Fig. 6c). For EG4, however, $\gamma \rightarrow \beta$ is multivalued. This is due to the fact that the amplitude of the compass deviation was as large as 100°. This means that there is even a reversal of the compass response, that is, when the correct heading is increasing, the uncorrected heading is actually decreasing: $(\partial\gamma/\partial\beta) < 0$ (green curve in Fig. 7b). The compass is extremely sluggish. In this region, the compass only traced a small range of directions ($\approx 55°$), but because of the sluggishness, this actually corresponds to a much wider range ($\approx 185°$) of correct instrument headings. The lookup table (Fig. 7c) to convert an uncorrected heading γ to the correct heading β is then simply the inversion in the sluggish region. The scatter in Fig. 7a would also suggest using

a linear fit. However, this would result in ambiguities; for example, $\beta = -180°$ would be mapped to $\beta - \gamma \approx -310°$ and $\beta = 180°$ would be mapped to $\beta - \gamma \approx 150°$, which, even taking into account the 360° periodicity, are completely different values. How would one then choose the correct one? Rather than using such a visually suggested linear fit, the fit to Eq. (1) provides a physically based recipe for applying a compass correction. The semicircular contribution to the compass deviation curve [parameters B and C in Eq. (1)] clearly is large, but as mentioned before, it is not possible from this to assess whether the compass deviation due to hard or soft iron was more severe. The fact that there are only a few instrument headings outside of this $\approx 185°$ range of correct headings is due to the fact that the mooring was embedded in a mostly unidirectional flow (actually a narrowband variability around that major direction), and that the ADCP representing the biggest asymmetric drag on the otherwise symmetric sphere was almost always located in the wake of the sphere, consistent with the orientation of any asymmetric blunt object in a flow.

The success of the method can be judged by comparing the current directions determined by the upper ADCP before and after the compass correction to the current directions determined by the lower instrument. The compass correction in the case of EG2 is minor, meaning that the histograms of the headings (Fig. 8a) and current directions (Fig. 8b) of the upper instrument do not change much and agree well with the lower current direction. This is also obvious in the scatterplot (Fig. 8c), where one would conclude that both the uncorrected and the corrected upper current directions reasonably agree with the lower current directions. However, the effect is relevant for EG4. The histogram for the headings (Fig. 9a) shows the increase of the range of headings from the uncorrected to the corrected situation and also the extremely sluggish behavior of the compass. The long tail of the uncorrected headings γ is to the left of the peak, while it is to the right of the peak of the corrected headings β. This is due to the fact that the correct heading actually decreases for an increase in the uncorrected heading (Fig. 7b). The histogram of the upper uncorrected current directions (Fig. 9b) has little resemblance to the lower current directions, while the agreement is much improved with the correction. This is also true for the direct scatterplot (Fig. 9c), where a majority of the scatter now falls in the vicinity of the straight line that would be applicable if there were no compass deviation, or conversely if the correction were perfect. The method is not perfect, but it leads to a much improved determination of the upper current direction.
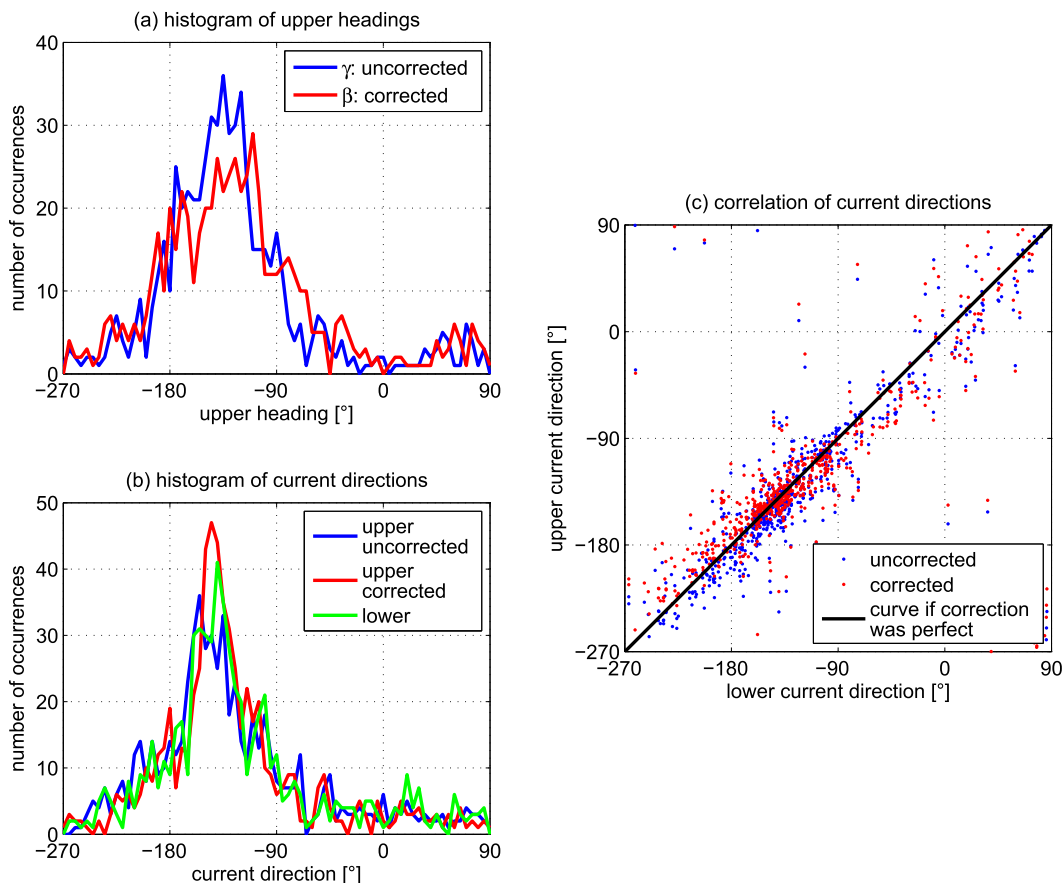
FIG. 8. Results of the compass correction of the ADCP on EG2. (a) Histograms of the headings before and after the correction, (b) histograms of the lower and upper current directions, and (c) scatterplot of the upper vs lower current direction. Since the compass deviation is small, the blue and red curves are close to each other. Note that the plotting limits of the periodic *x* axis are chosen to best fit the histograms into the interior of the figure.

However, the developed method fails to determine the correct instrument heading for some recorded uncorrected instrument headings located outside of the invertible region of the fitted curve (Fig. 7a). For those headings, a correction of the velocity is not possible. This leads to a biased (as a function of instrument heading and therefore most likely current direction) exclusion of data. While this is unfortunate, the method uses a physically justified procedure to determine the correct current direction for the majority of the top ADCP data. For 7873 hourly records at mooring EG4, the compass directions could successfully be corrected and the correction failed in 13% of the measurements. For the other moorings, the failure rate ranged from 0% to 30%. Since there were many times when only the upper ADCPs recorded velocity (e.g., because the MMPs only sampled twice a day and were sometimes stuck at depth, while the ADCPs sampled hourly), this method made large amounts of data usable in addition to the overlapping recordings.

5. Conclusions

A method has been described to correct velocity measurements affected by compass deviations caused by iron in the instruments' proximity. It is likely that errors to oceanic velocity measurements due to compass deviations are rather frequent, although the amplitudes may be smaller than the ones presented here. This should therefore be considered in the error discussion of oceanic velocity measurements. Where overlapping uncompromised measurements are available, the method (including the ready-to-use MATLAB function described in the appendix) presented here may be used to improve data quality or to make data usable in the first place.

While this paper has focused on correcting the compass deviation after data acquisition, we would also like to raise awareness of the problem in the first place. This will hopefully help to limit these problems during the mooring design phase. Physically separating compasses from large bodies of iron such as steel spheres is the most effective
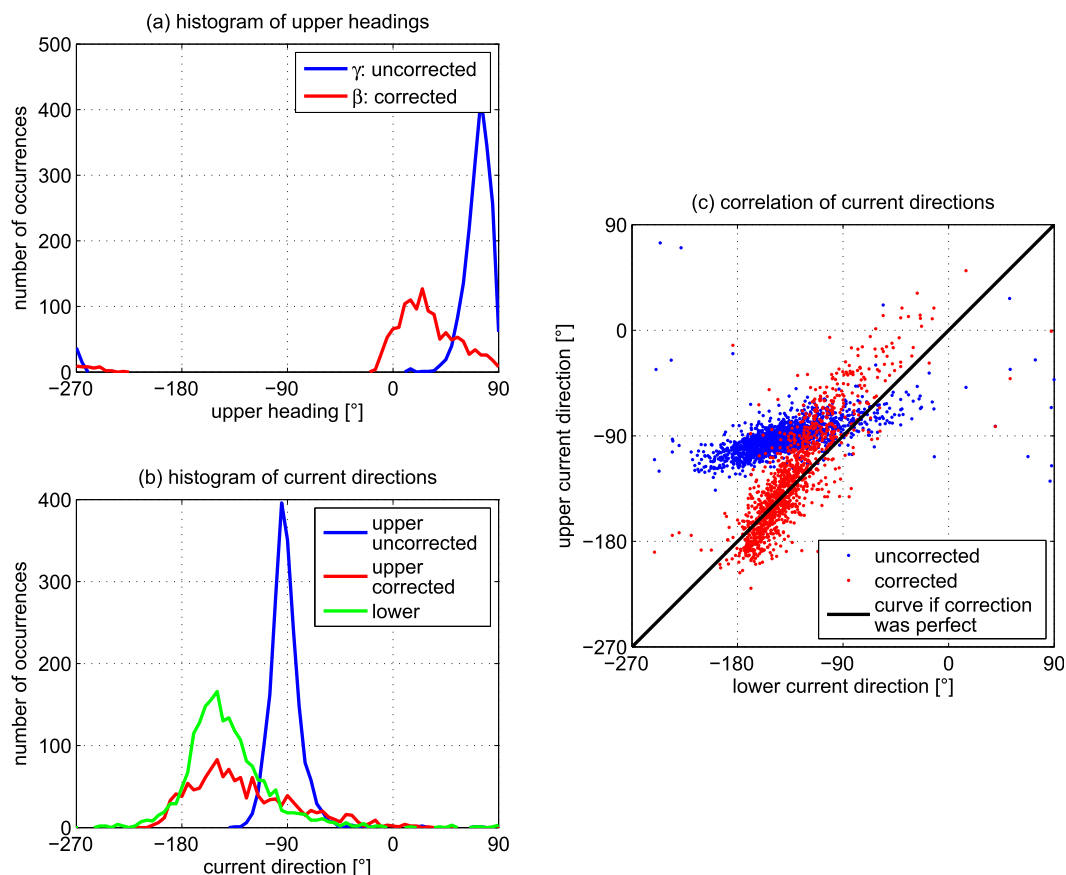
FIG. 9. As in Fig. 8, but for EG4. Since the compass deviation is large, the blue and red curves differ significantly, and the improvement in the correlation (c) is indicative of the success of the compass correction.

way to avoid compass deviations. Even a separation by a few meters is highly beneficial. If a physical separation is not possible, then it is advised to test for the compass deviation prior to deployment and possibly to choose configurations with smaller amplitude compass deviations.

APPENDIX

Description of MATLAB Function and Example Data Available Online

The supplemental online material (http://dx.doi.org/10.1175/JTECH-D-14-00043.s1) contains a MATLAB function called compass_correction.m that implements the method described in the paper. It is accompanied by two functions, plot_analysis.m and plot_results.m, that plot the compass correction curve and provide an assessment of the success of the correction, respectively. The nonlinear least squares fit to Eq. (1) is achieved using the MATLAB curve-fitting toolbox. An open source alternative is to use curve_fit from Python's scipy.optimize package for this part of the calculation or the whole calculation. However, because MATLAB is commonly used in the oceanographic community, we only provide a MATLAB function here. The help of compass_correction.m provides a usage example that can be directly executed from the MATLAB command prompt.

The average velocity and depth of the first two bins above the upper ADCP was taken at the measurement times (hourly sample rate). The same was done for two bins of the lower current meter. These depths varied over time due to vertical mooring motion. All the measurements from the two instruments that were separated by less than 20 min in time and 20 m in the vertical were considered to be overlapping. By not using a fixed depth below the surface, this also explicitly incorporates times when the moorings were blown down significantly. The

overlapping records from all seven moorings were then interpolated onto the same hourly grid returning NaNs where no data were within ±30 min of the temporal grid. These data from the seven moorings are also supplied for testing of the MATLAB function. Its file name is example_vels.mat.

REFERENCES

Harden, B., R. Pickart, and I. A. Renfrew, 2014: Offshore transport of dense water from the East Greenland shelf. *J. Phys. Oceanogr.,* **44,** 229–245, doi:10.1175/JPO-D-12-0218.1.

National Geospatial-Intelligence Agency, 2004: Handbook of magnetic compass adjustment. National Geospatial-Intelligence Agency Tech. Rep., 45 pp. [Available online at http://msi.nga.mil/MSISiteContent/StaticFiles/HoMCA.pdf.]

von Appen, W.-J., and Coauthors, 2014a: The East Greenland Spill Jet as an important component of the Atlantic Meridional Overturning Circulation. *Deep-Sea Res. I,* **92,** 75–84, doi:10.1016/j.dsr.2014.06.002.

——, R. Pickart, K. Brink, and T. W. N. Haine, 2014b: Water column structure and statistics of Denmark Strait Overflow Water cyclones. *Deep-Sea Res. I,* **84,** 110–126, doi:10.1016/j.dsr.2013.10.007.